

# Connecting phenological predictions with population growth rates for mountain pine beetle, an outbreak insect

James A. Powell · Barbara J. Bentz

Received: 21 July 2008 / Accepted: 7 March 2009 / Published online: 3 April 2009  
© Springer Science+Business Media B.V. 2009

**Abstract** It is expected that a significant impact of global warming will be disruption of phenology as environmental cues become disassociated from their selective impacts. However there are few, if any, models directly connecting phenology with population growth rates. In this paper we discuss connecting a distributional model describing mountain pine beetle phenology with a model of population success measured using annual growth rates derived from aerially detected counts of infested trees. This model bridges the gap between phenology predictions and population viability/growth rates for mountain pine beetle. The model is parameterized and compared with 8 years of data from a recent outbreak in central Idaho, and is driven using measured tree phloem temperatures from north and south bole aspects and cumulative forest area impacted. A model driven by observed south-side phloem temperatures and that includes a correction for forest area previously infested and killed is most predictive and generates realistic parameter values of mountain pine beetle fecundity and population growth.

Given that observed phloem temperatures are not always available, we explore a variety of methods for using daily maximum and minimum ambient temperatures in model predictions.

**Keywords** Mountain pine beetle · *Dendroctonus ponderosae* · Growth rate prediction · Phenology · Temperature change · Insect outbreak

## Introduction

We currently face an era of climate change, manifested as a trend of generally increasing temperature. In the western US, for example, mean annual temperatures have increased by 2°C since 1984 across all latitudes (IPCC 2007). Climate model predictions indicate that this trend is likely to continue at least through the middle of the twenty-first century. While there are clear abiotic impacts, including retreat of glaciers, rising sea levels, and unpredictable changes in precipitation, impacts on biological systems are equally significant.

The vast majority of organisms are ectotherms, with body temperatures directly controlled by their surroundings. For these organisms the very pace of life is a function of temperature. For temperate ectotherms in particular, thousands of generations in relatively consistent climatic conditions have resulted in adaptation of each species' thermal responses to its

---

J. A. Powell (✉)  
Department of Mathematics and Statistics, Utah State  
University, Logan, UT 84322-3900, USA  
e-mail: jim.powell@usu.edu

B. J. Bentz  
USDA Forest Service, Rocky Mountain Research Station,  
Logan, UT 84321, USA  
e-mail: bbentz@fs.fed.us

local niche and habitat (Taylor 1981). This adaptation to local environments is termed seasonality, and often involves timing that leads to cycles of activity in important life history traits that may be under direct temperature control (Danks 1987) or cued by a biofix such as diapause (Zaslavski 1988). Regardless of the mechanism, temperature-driven adaptation is a major determinant of ectotherm success. For example, the timing of hibernation, quiescence and diapause can increase the probability that extremes of drought and temperature are avoided (Tauber et al. 1986). Simultaneous emergence can also be adaptive as it is advantageous for finding mates and avoiding predators (Calabrese and Fagan 2004), and is often timed with ephemeral resources, as when bees specialize on the pollen of specific plants (Brody 1997), or larval feeding on new foliage in the spring (Hunter and Elkinton 2000). The timing of other activities, such as oviposition, may need to occur prior to extreme cold, but late enough to insure that offspring survive cold periods in diapause or a cold-hardened state (Bale 2002). For many species a degree of variability in timing is adaptive (Friedenberg et al. 2007), either as a bet-hedging strategy against the variability of environmental events or to ensure temporal coverage of unpredictable resources (Post et al. 2001). Because the consequences of poor timing are extreme for temperate ectotherms, life history event timing is highly evolved, specialized for the requirements of individual species, and depends strongly on environmental signals, particularly temperature. Due to this dependency on temperature we may expect that a significant impact of global warming will be a disruption of these traits as environmental cues become disassociated from their selective impacts. In fact, insect species that outbreak are predicted to be heralds of severe ecological consequences because their population growth often depends on release from environmental constraints (Logan et al. 2003).

The mountain pine beetle (MPB, *Dendroctonus ponderosae*, Coleoptera: Curculionidae, Scolytinae, Hopkins) infests and kills *Pinus* host trees throughout western North America, and rapid population growth and inherent positive feedbacks are hallmarks of this economically important species (Raffa et al. 2008). The MPB geographical distribution generally reflects that of its primary hosts, although the range of lodgepole pine (*Pinus contorta* Douglas) extends further to the north and other pine species further to

the south than where MPB populations currently exist. Unlike most phytophagous insects, successful MPB reproduction requires death of all or part of the host. Host trees, however, have evolved effective resin response mechanisms to defend themselves against bark beetle attacks (Raffa et al. 1993; Lieutier 2002). Almost all trees are capable of responding to bark beetle attacks, but only those with a rapid and sustained response are likely to survive. If many beetles attack the same tree over a short period of time (e.g., mass attack) they can exhaust the host's defensive mechanisms. The final outcome of a bark beetle dispersal and colonization attempt is, therefore, dependent upon a series of competing rate reactions which regulate both beetle arrival and host tree resin response (Safranyik et al. 1989; Raffa and Berryman 1983). This evolved relationship has resulted in an elaborate semiochemical communication system through which adult beetles use host tree chemistry to draw conspecifics to the tree (Borden 1974). To be successful, however, peak emergence from brood trees must be synchronous, thereby ensuring a sufficient number of adults for mass attack of new host trees (Reid 1962a; Logan and Bentz 1999). Like other ectotherms, developmental timing and synchronous adult emergence in MPB is a direct result of temperature (Safrayik et al. 1975; Bentz et al. 1991; Logan and Bentz 1999).

The MPB has been successful across a broad spectrum of latitude and temperature regimes as measured by the numerous population outbreaks recorded the past 100 to 150 years across western North America (Crookston et al. 1977; McGregor 1978; Perkins and Swetnam 1996; Alfaro et al. 2004). However, the severity and distribution of some recent outbreaks differ from what can be inferred from historical records, and increasing temperature associated with climate change is believed to be a significant factor in these population outbreaks (Logan and Powell 2001; Carroll et al. 2004; Aukema et al. 2008). Phenology models that describe the effect of temperature on MPB developmental timing have been developed and can be used for analyzing MPB response to historic and future climate regimes (Bentz et al. 1991; Logan and Bentz 1999; Powell et al. 2000; Gilbert et al. 2004). One variant of the phenology model has been used to infer suitable thermal habitat and thus long-term population success based on probabilities of appropriate timing and seasonality

(Hicke et al. 2006). Although when used in this fashion the model provides a relative risk of outbreak, it is not intended to be an outbreak predictor or measurement of population growth potential. Outbreak predictions depend on understanding population growth rates, and thus upon a demographic model.

There is a long history of demographic population modeling, some of it specific to mountain pine beetle (Berryman et al. 1984; Berryman et al. 1989; Powell et al. 1996; Logan et al. 1998; Heavilin and Powell 2008; Nelson and Lewis 2008). However, very little of this modeling explicitly includes the interaction between phenology, temperature, and population success as manifested by quantitative dependence of demographic parameters on environmental variables controlling life history traits. Exceptions include the work of Xia et al. (2003), who explicitly include temperature and phenology in field models of predator/prey interactions of ladybird beetles with aphids as well as Logan et al. (2006), who include the effect of temperature on arthropod predators. Aukema et al. (2008) have also linked temperature and MPB dynamics with landscape-scale spatial and temporal dependencies to explain outbreak probabilities. Predictions of significant temperature increases over the next century highlight the need for continued development of quantitative connections between insect population demographics and the relationship between climate and phenology.

In this paper we connect a distributional model for MPB phenology to a mathematical framework that describes population success at a landscape scale, bridging the gap between tree-level phenology predictions and population growth rates for MPB. The model is parameterized using aerial survey data of trees killed by MPB and is driven using measured temperature of the tree phloem in which MPB develop. We discuss a variety of models that can be used to estimate phloem temperature from daily maximum and minimum ambient temperature records and their effect on growth rate predictions.

## Model development

### Distributional model for phenology

Insect developmental models seek to determine how temperature ( $T$ ) influences the time required to complete each life stage of development. Median

development rates, as a function of temperature ( $r(T)$ ), of MPB oviposition, egg hatch, larvae (four stages), pupae, and callow adult have been estimated (Bentz et al. 1991; Logan and Bentz 1999). The functional forms and best-fit parameters for these relationships appear in Gilbert et al. (2004). At every temperature, individuals develop at slightly different rates from one another, generating a distribution of development times. Following Gilbert et al. (2004) the density of individuals,  $p$ , at physiological age,  $a$ , at time,  $t$ , obeys an extended von Foerster (EvF) equation

$$\frac{\partial p}{\partial t} + r(T(t)) \frac{\partial p}{\partial a} = v(T(t)) \frac{\partial^2 p}{\partial a^2}.$$

The parameter,  $v$ , which could itself depend on temperature but which we take as constant in each life stage [see Gilbert et al. (2004) for justification] is proportional to the variance in development expressed at each temperature. When there is no variability ( $v = 0$ ) this equation causes each individual to age at a rate,  $r$ , which depends directly on temperature at any given time,  $T(t)$ . Thus, in any particular life stage an individual requires  $t_{\text{end}} - t_{\text{beg}}$  amount of time to emerge, where the beginning ( $t_{\text{beg}}$ ) and end ( $t_{\text{end}}$ ) times of the stage are related by

$$1 = \int_{t_{\text{beg}}}^{t_{\text{end}}} r(T(t)) dt$$

as described in Powell and Logan (2005). When  $v$  is non-zero it leads to a mixing of individuals in ages relative to the median rate of development,  $r(T(t))$ . That is, some individuals age more slowly than the mean while others age more rapidly. This mixing could vary with either temperature or rate, but for MPB the most predictive model is constant across temperature and rate. Values of  $v$  for all MPB life stages appear in Gilbert et al. (2004).

For a given temperature record, calculation of a distribution of emergence times (at which  $a = 1$ , or insects are fully matured in their life stage) may be accomplished using the Green's function solution,

$$G(t, \tau) = \frac{1 - r(T(t))}{\sqrt{4\pi v(t - \tau)^3}} \exp\left(-\frac{(1 - \int_{\tau}^t r(T(x)) dx)^2}{4v(t - \tau)}\right),$$

which can be interpreted as the probability density function (pdf) of development, in emergence time,  $t$ ,

for an individual starting development in a particular life stage at time  $\tau$ . The variable,  $x$ , appearing in the integral is a dummy variable of integration; the integral accounts for the total amount of development occurring for the median individual between  $\tau$  and  $t$ .

The Green's function can be derived from the EvF starting with boundary conditions  $p(a = 0, t) = \delta(\tau)$  and  $p(a, t = 0) = 0$ , corresponding to a single egg laid at time  $\tau$ . We introduce a change of variables to a frame of reference moving with the median individual,

$$z = a - \int_{\tau}^t r(T(x)) dx.$$

The EvF becomes

$$\frac{\partial p}{\partial t} = v \frac{\partial^2 p}{\partial z^2},$$

$$p(z = 0, t) = \delta(t - \tau), \quad p(z, t = 0) = 0.$$

Taking the Laplace transform in  $t$  gives

$$sP = vP'', \quad P(z = 0) = e^{-s\tau}.$$

Here  $P(z, s)$  is the Laplace transform of  $p(z, t)$  and primes denote differentiation with respect to the  $z$  variable. Solving this differential equation gives

$$P(z, s) = e^{-s\tau - |z| \sqrt{sv}}.$$

Inverting the Laplace transform,

$$p(z, t) = \frac{|z|}{\sqrt{4\pi v(t-\tau)^3}} \exp\left[-\frac{z^2}{4v(t-\tau)}\right]$$

$$= \frac{|a - \int_{\tau}^t r(T(x)) dx|}{\sqrt{4\pi v(t-\tau)^3}} \exp\left[-\frac{\left(a - \int_{\tau}^t r(T(x)) dx\right)^2}{4v(t-\tau)}\right].$$

The end of the life stage occurs when  $a = 1$ ; thus

$$p(t, \tau) = \frac{1 - r(T(t))}{\sqrt{4\pi v(t-\tau)^3}} \exp\left[-\frac{\left(1 - \int_{\tau}^t r(T(s)) ds\right)^2}{4v(t-\tau)}\right]$$

$$= G(t, \tau),$$

which is the Green's function above. Consequently, the distribution of emergence,  $p_{out}(t)$ , for a life stage with input distribution  $p_{in}(\tau)$  can be calculated using convolution,

$$P_{out} = \int_0^t G(t, \tau) P_{in}(\tau) d\tau.$$

That is, for each starting day,  $\tau$ , the pdf,  $G(t, \tau)$ , of emergence times for eggs starting on  $\tau$  is integrated against the density of eggs for all possible  $\tau$ , generating a density of eggs emerging at time  $t$ . By daisy-chaining these convolutions (the output of the previous life stage becoming the input distribution for the subsequent life stage) a distribution of adult emergence for the next generation can be calculated based on distributions of adult emergence in the current generation.

### Beetle effectiveness

How does a distribution of adult emergence translate into population success, given the requirements of seasonality and synchronous emergence? Two factors must be considered: (1) the number of adults in a generation produced by an adult in the previous generation (net survivorship,  $s$ , times fecundity,  $f$ ) and (2) the number of emerging MPB on a daily basis required to successfully overcome host tree defenses (attack threshold,  $A$ ). *Effective* beetles,  $E_n$ , in a distribution are those which manage to exceed the daily threshold,

$$E_n = \int_{152}^{245} \max(sf P_n(t) - A, 0) dt,$$

where  $f$  is the number of eggs laid for all females in a tree,  $s$  is the fraction of those eggs surviving to emergence,  $A$  is the number of MPB required on a daily basis to successfully infest a tree, and  $P_n(t)$  is the density of adult emergence associated with a tree in year  $n$ . The limits of integration, 152 and 245, correspond to reasonable limits on seasonality; development of eggs laid earlier than June 1 or later than August 30 will not be in the proper life stage (larvae or brood adult) to survive fall and winter cold temperatures (Bentz and Mullins 1999; Régnière and Bentz 2007).

### MPB infestation data in the Sawtooth National Recreation Area

The Stanley valley of the Sawtooth National Recreation Area (SNRA) in central Idaho was chosen as our study area for several reasons. A single host, lodgepole pine, predominates, and host demographics

are consistent across the valley due to historical disturbance patterns. Lodgepole pine stands in the SNRA are within a coherent geographic unit, bounded by 3,000+ m mountains on three sides, minimizing factors such as dispersal and immigration that have been shown to be important in MPB outbreaks (Aukema et al. 2008). The valley opens to the north, cross-wise to prevailing weather patterns, and is small enough that the entire valley experiences the same general climate. Finally, the rate curves which describe MPB phenology model were parameterized from a population in this area, removing one source of potential uncertainty.

Estimates of the number of MPB-attacked trees in the SNRA were derived from Aerial Detection Surveys (ADS) conducted by USDA Forest Service, Forest Health Protection (<http://www.fs.fed.us/r1-r4/spf/fhp/aerial/gisdata>). Surveys are conducted in

fixed-wing aircraft wherein observers delineate areas of trees with faded foliage, presumed to have been attacked and killed by MPB the previous year. Although the rate of foliage fading may vary among years and geographic areas, observers are trained to distinguish among tree colors and we assume the data reflects MPB-caused tree mortality with a 1-year lag. Only areas with at least 20 trees/ha were mapped. The data were entered into a GIS database and the number of hectares attacked and killed by MPB per year estimated. For this study, the area used is 31.5 km in north/south extent by 56.3 km in east/west directions (Fig. 1).

Although aerial survey information has inherent errors such as spatial location errors and discerning host versus non-host tree species, data of this type have proven useful for studying mountain pine beetle population trends at the landscape level (Aukema

**Fig. 1** Region of Aerial Detection Survey coverage in 2002 for the Sawtooth National Recreation Area (SNRA) in central Idaho. Shown are trees attacked by MPB in 2001, lakes (in darkest shading), and the location of two research sites where phloem temperatures were collected. The lower left corner of the map is ~35 km south and 15 km west of the town of Stanley. The total area covered is ~1,773 km<sup>2</sup>, of which 333 had aeri-ally-detected MPB infestation

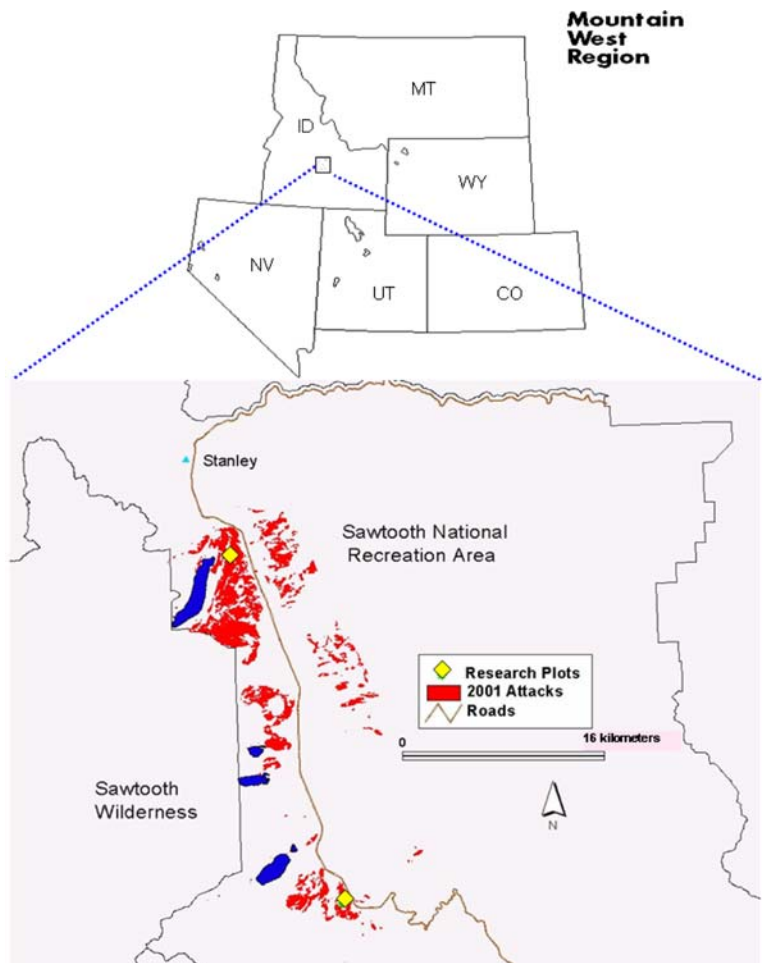


**Table 1** Area of lodgepole pine impacted by mountain pine beetle and population growth rates in the study area

Year	Area	$r_n$
1989	18.5	–
1990	32.1	1.74
1991	7.95	.248
1992	22.5	2.83
1993	1.15	.0512
1994	4.71	4.10
1995	3.56	.755
1996	6.14	1.72
1997	8.12	1.32
1998	15.1	1.86
1999	33.2	2.20
2000	83.7	2.52
2001	171	2.04
2002	333	1.95
2003	521	1.56
2004	576	1.10

Area impacted is reported in square kilometers; growth rates ( $r_n$ ) are the ratio of impacted areas between years  $n$  and  $n-1$

et al. 2006). In our study area the major MPB host tree, lodgepole pine, grows in stands with relatively homogenous demographics at the lowest elevations. A variety of other conifer species (but no pine hosts until much higher altitude) are found as elevation increases. To ensure only areas of host trees were included in the analyses, observed ADS data was rasterized to a  $30 \times 30$  m resolution and masked using a lodgepole pine vegetation map (USDA Forest Service, Sawtooth National Forest) at the same spatial resolution. Areas impacted by MPB per year and related estimates of population growth rates are presented in Table 1.

#### Estimating parameters

We make the assumption that the number of trees per ha is relatively constant, and therefore the area growth rate is precisely the growth rate in population of infested trees. Although demographic information on host densities is not available in a spatially distributed fashion throughout the study area to validate this assumption, disturbance history in the area has resulted in relatively homogenous lodgepole pine stands. Additionally, we incorporate variance

from this assumption in the likelihood error discussed below. If  $H_n$  is the number of observed hectares of infested trees in year  $n$ , the observed growth rate is

$$r_n = \frac{H_n}{H_{n-1}}.$$

We fit the model

$$r_n = \alpha E_n \cdot \exp\left(-\beta \sum_j^{n-1} H_j\right)$$

to these observations, where  $\alpha$  may be interpreted as the predicted number of hosts colonized per ‘effective’ MPB (described below) and the exponential factor is an area correction term which decrements population growth rates according to the total hectares of trees killed by MPB in previous years. This term represents the probability of infesting beetles being able to encounter new susceptible trees in a Poisson search process, with  $\beta$  denoting the failure rate per ha. This amounts to a three-parameter model linking phenology to population growth, since three of the four apparent parameters affect the model only in the combination  $a_1 = \alpha \cdot sf$  and  $a_2 = \alpha A$ . One of the parameters can be set to an arbitrary reference value; we choose to set the threshold for effective beetles ( $A$ ) to 250, corresponding to 40 MPB/m<sup>2</sup> per day required to overcome a tree (Raffa and Berryman 1983), projected 6.25 vertical meters above ground for a 32 cm diameter at breast height (DBH) tree. Trees of this size are approximately the average size of those attacked by MPB in the SNRA.

Predicting emergence distributions in a given year depends on two factors whose effects are difficult to assess: the temporal distribution of successful attacks the previous year (generally unmeasured) and the temperature in the developmental environment. As an input distribution of attacks we assume normal with mean day of emergence JD 205 (July 24, except in leap years), based on data in Bentz (2006), and a standard deviation of 5 days. Sensitivity to these assumptions is discussed in the Results.

Temperature distributions are more problematic. The developmental environment of MPB is the phloem of pine trees, which is often significantly warmer than ambient temperatures, particularly on the southern bole aspects due to radiant solar input. Northern bole aspect temperatures track ambient temperatures with a short time lag, although they are

occasionally slightly higher than ambient, possibly due to re-radiation of solar energy from the surroundings. MPB develop and emerge on all aspects of a tree equally well (Rasmussen 1974; Bentz 2006). We investigated the effect of temperature on population growth rates using data from both northern and southern bole aspects, as well as temperatures averaged for both bole aspects. Phloem temperatures were from a total of 12 MPB infested-lodgepole pines at multiple sites throughout the SNRA, collected sequentially (Bentz unpublished data). We refer the reader to (Bentz 2006) for details on temperature measurements. Phloem temperature measurements were taken from different infested trees in sequential years and combined to form a continuous thermal record from JD 200 in 1992 to JD 289 in 2004.

A model for population growth rate using effective MPB ( $A = 250$ ), and the same model with a correction factor for hectares previously impacted (thus removed from potential host status) were fit to observed area growth rates using nonlinear maximum likelihood (equivalent to least square error with unknown variance also estimated, Burnham and Anderson 2002) for each 12 year temperature series from the north, south and averaged bole aspects. Objective functions based on absolute and logarithmic errors did not give appreciably different results.

## Results

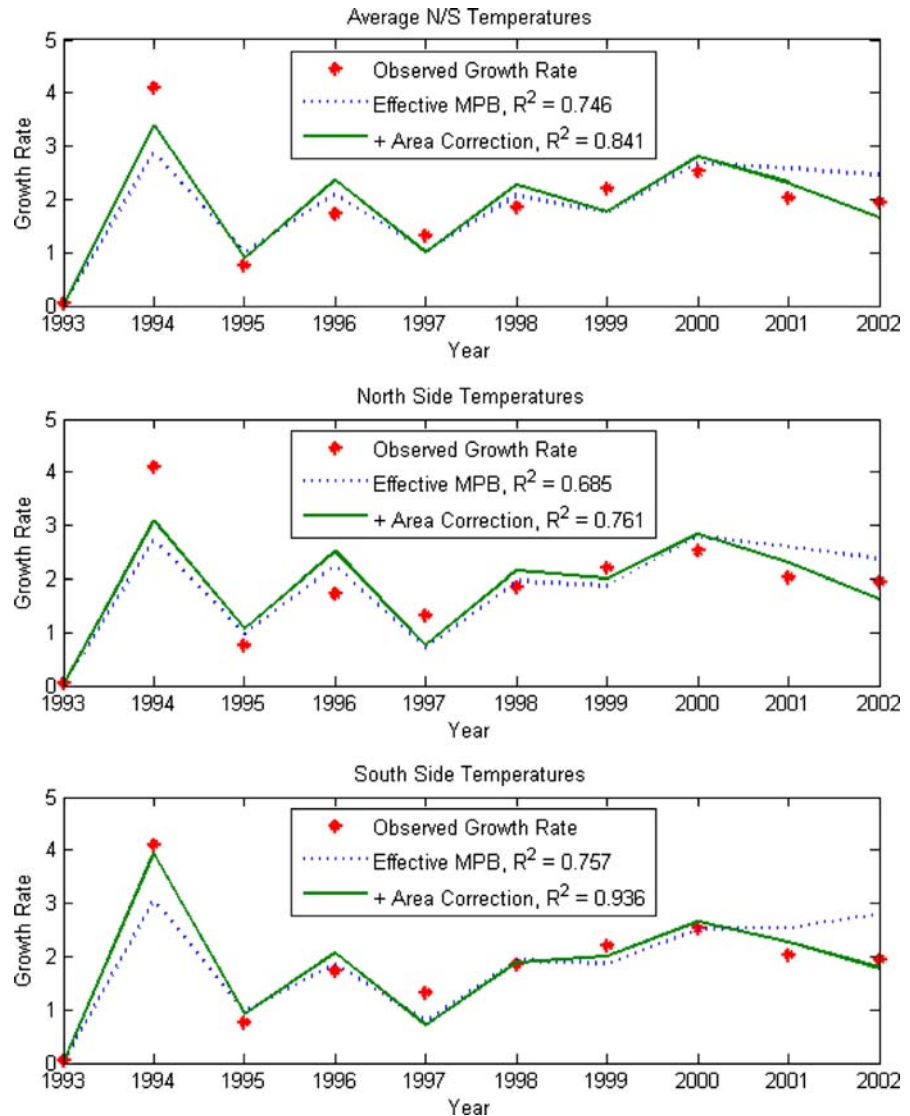
Among all models, use of south-side tree bole temperature provided the best fit ( $r^2 = 93.6\%$ ) to observed growth rates, as measured by correlation coefficients (Fig. 2). Sensitivity analyses with respect to both date of peak of emergence (in the range JD 190–220) and duration of initial attack (standard deviation in the range 1–10 days) revealed only a 1% change in results. Analysis of the significance of these differences will be discussed below. All models did a good job of tracking the fluctuations of observed population growth rates, although models with no area correction ( $\beta = 0$ ) performed poorly after 2000 as available hosts declined (Fig. 2). The annual variability in growth rates was captured surprisingly well by the models due to differences between the thermal signature, and therefore the emergence pattern, in differing years.

Predicted adult emergence patterns in 1995 and 2001 are compared in Fig. 3. In each of these years the south-side phloem temperature model + area correction matched the observed growth rates of 0.755 in 1995 and 2.04 in 2001 very closely. Parameter estimates for each year suggest  $\sim 11,000$  beetles emerging between JD 180 and 245. Predicted emergence was more dispersed in 1995 than 2001, and the number of MPB exceeding the daily threshold and killing new trees was less than half as much in 1995 as 2001. This resulted in a difference in predicted growth rates between those 2 years. Differences between the models with and without area correction ( $\beta > 0$  vs.  $\beta = 0$ ) can be seen most clearly in the latter years, where there was a general decline in growth rates from 2000 through 2002. Models with only temperature ( $\beta = 0$ ) do not capture this trend, and accuracy earlier in the time series was diminished.

Best-fit parameter values for the various models and temperature series are presented in Table 2. Computationally the combined parameters,  $a_1 = \alpha \cdot sf$  and  $a_2 = \alpha A$ , as well as the parameter  $\beta$  which is the rate at which growth rates are decremented by previously infested areas (area correction term), were estimated, and confidence intervals (using parametric bootstrapping, described below under Analysis of Significance) are reported for these parameters. Because  $a_1$  and  $a_2$  are difficult to biologically interpret, we include in Table 2 corresponding estimates for net fecundity of an infested tree and the total number of effective MPB (that is, net number produced over the threshold  $A$ ) that are required to successfully overcome a new host tree. To obtain these parameters from the estimates required choosing an exogenous parameter; we chose  $A = 250$  for a threshold value, corresponding to the threshold number of beetles required to achieve a threshold of 40 MPB/m<sup>2</sup> (Raffa and Berryman 1983) on a tree of 32 cm diameter over the lower 6.25 m of bole.

For models using south-side temperatures this resulted in a gross productivity of  $\sim 11,000$  MPB per infested tree. These models estimate a total of 1,380 MPB infesting a new tree, which means the net per beetle fecundity predicted is 8.1 female survivors per infesting female *within* the tree, not accounting for beetles that die between trees or fail to overcome the daily threshold during attack. Phloem temperatures averaged across north and south boles

**Fig. 2** Graphical comparison of observed MPB population growth rate (\*) in the SNRA study area, and models predicting population growth rate as a linear function of effective MPB (*dashed line*), and with a correction for previously infested area to growth rates (*solid line*). Effective MPB are the net number of beetles produced over a set daily threshold (see text), directly proportional to predicted growth rates. For all models, south-side temperatures provided better predictions for observed growth rates. Inclusion of both effective MPB and a correction for previously infested area provided the best prediction of population growth rates, accounting for over 93% of observed variability



generate comparable numbers; 14,400 net MPB/tree and 2,240 MPB to infest a new tree, giving a net fecundity of 6.4 per infesting female. Models using north side phloem temperatures were almost as predictive as models using south side and average temperature, resulting in a net fecundity of 4.5 per infesting female. Given that an average female can lay between 50 and 100 eggs (Reid 1962b), these numbers correspond to mortalities in the vicinity of 90–95%, which correspond favorably with numbers reported by Amman and Cole (1983).

Including an area correction term for areas infested in previous years improves model predictions of

population growth rate, regardless of temperature profile used. The parameter  $\beta$  controls the rate of growth rate decrease with total area previously infested, and is related to the inverse of the 'carrying capacity', which would be  $K = \ln(\alpha)/\beta$ . This  $K$  would be the area of hosts attacked that would cause the net growth rate in the subsequent generation to be one. For the model using south-side temperatures, this carrying capacity is estimated at  $6.63 \times 10^5$  ha. Averaged north- and south-side phloem temperatures give  $K = 7.76 \times 10^5$  ha, and north-side temperatures predict a carrying capacity of  $7.17 \times 10^5$  ha. Summing total lodgepole pine area (based on the vegetation map)

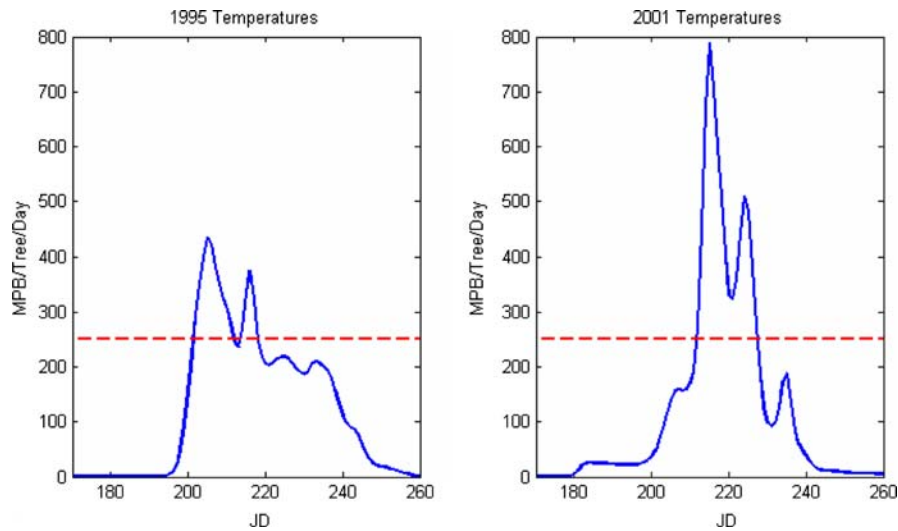


**Fig. 3** A comparison of predicted MPB emergence distributions in 1995 and 2001 in the SNRA study area. In each year, 11,000 MPB were distributed under the emergence curve between JD 180 and 260, but differences in temperatures between the 2 years resulted in differences in timing and

synchrony of adult emergence. The reference threshold for attack, 250 MPB/tree day<sup>-1</sup>, is shown. The net number of MPB exceeding this threshold (e.g., effective beetles) in 2001 is twice that in 1995, resulting in predicted population growth rates of 2.04 in 2001 and 1.03 in 1995

within the study area gives  $7.1 \times 10^5$  ha, which compares favorably with all three estimates for *K*.

Analysis of significance

Significance of these results and parameter confidence intervals were developed using bootstrapping on the spatial data and corresponding changes in the Akaike Information Criterion (AIC, Akaike 1978). Least-squares fitting amounts to an application of maximum likelihood with

$$r_n = \alpha E_n \exp\left(-\beta \sum_j^{n-1} H_j\right) = \frac{H_n}{H_{n-1}} + \varepsilon_n,$$

where  $\varepsilon_n$  is an error term with normal distribution, zero mean, and an unknown variance,  $\sigma$ . Among other effects, this error term accounts for variance in our predictions due to unmeasured variability in host density. The negative log likelihood (objective function to minimize) is

$$L = \frac{1}{2} \left[ N \log(2\pi\sigma^2) + \frac{1}{\sigma^2} \sum \left( r_n - \frac{H_n}{H_{n-1}} \right)^2 \right].$$

The AIC is then defined

$$AIC = 2(\text{Number of Parameters Estimated}) + L.$$

Changes in the AIC provide a way to compare models with differing numbers of parameters (Anderson et al. 2000) as well as structural differences (for example, using different temperature data). Small AIC corresponds to a better balance of model complexity and fit to the data, with more complex models penalized for their greater number of parameters.

To develop confidence intervals for parameters (reported above in Table 2) we bootstrap the original spatial data. For each year a single bootstrap sample is generated by choosing individual  $30 \times 30$  m area elements from the ADS data at random, with replacement, and tallying the number of infested hectares. This procedure was repeated  $10^4$  times for each year of data, generating  $10^4$  bootstrapped time series of impacted areas. Parameters were fit to each of these series for all six models (northern, southern or averaged phloem temperatures crossed with presence or absence of a cumulative area correction term), and for each fit an AIC was calculated. The minimum AIC over all models and bootstrapped samples was used as a reference value to compare models via differences in AIC as suggested by Burnham and Anderson (2002),

**Table 2** Model parameters determined using nonlinear regression, based on north, south and averaged phloem temperatures of host trees

	South side temperatures		South side temperatures + area correction	
	Estimate	95% CI	Estimate	95% CI
$a_1$	8.10	(7.05, 8.36)	12.2	(11.9, 12.6)
$a_2$	0.181	(0.141, 0.191)	0.313	(0.299, 0.327)
$\beta \times 10^6$ (ha <sup>-1</sup> )	–	–	10.8	(10.5, 11.1)
$sf$ (MPB/tree)	11,200	(10,900, 12,500)	9,760	(9,610, 9,930)
$1/\alpha$ (Effective MPB/tree)	1,380	(1,310, 1,770)	798	(765, 835)
$R^2$ (%)	75.7		93.6	
	Average temperatures		Average temperatures + area correction	
	Estimate	95% CI	Estimate	95% CI
$a_1$	6.45	(6.05, 6.70)	8.38	(7.64, 8.94)
$a_2$	0.112	(0.0989, 0.119)	0.161	(0.138, 0.179)
$\beta \times 10^6$ (ha <sup>-1</sup> )	–	–	8.33	(7.70, 8.96)
$sf$ (MPB/tree)	14,400	(14,000, 15,300)	13,000	(12,500, 13,900)
$1/\alpha$ (Effective MPB/tree)	2,240	(2,090, 2,530)	1,550	(1,400, 1,810)
$R^2$ (%)	74.6		84.0	
	North side temperatures		North side temperatures + area correction	
	Estimate	95% CI	Estimate	95% CI
$a_1$	4.53	(4.25, 4.78)	5.22	(4.99, 5.58)
$a_2$	0.0455	(0.0387, 0.0512)	0.0538	(0.0620, 0.030)
$\beta \times 10^6$ (ha <sup>-1</sup> )	–	–	7.49	(6.95, 8.17)
$sf$ (MPB/tree)	24,900	(23,100, 27,500)	25,300	(22,500, 25,700)
$1/\alpha$ (Effective MPB/tree)	5,490	(4,830, 6,460)	4,650	(4,030, 5,150)
$R^2$ (%)	68.5		76.1	

The parameters  $a_1$  and  $a_2$  are dimensionless parameters related to the net fecundity of MPB-killed trees and attack thresholds, respectively. Easier to interpret is the combination  $sf$ , or net productivity of infested trees in terms of MPB, and  $1/\alpha$ , the estimated number of effective MPB per new host successfully attacked (after surpassing a threshold of 250 MPB/day). The parameter  $\beta$  controls the area correction to growth rate, decrementing according to the total number of hectares previously infested. The percent variance in observed growth rates explained by the corresponding model,  $R^2$ , is also reported

$$\Delta AIC = AIC_{\text{model}} - AIC_{\text{min}}$$

Low values of  $\Delta AIC$  correspond to better fits. Histograms of  $\Delta AIC$  are depicted in Fig. 4, and best fit results for all models and their relationship to  $\Delta AIC$  distributions appear in Table 3. Overall, the model produced based on south-side phloem temperatures and a correction for area previously infested produced the best AIC, and was significantly better than all competing models.

A similar analysis of significance can be performed on models that predicted population growth rate based

only on phloem temperatures (e.g., south-side, north-side, or averaged) without an area correction. The model based on south-side phloem temperatures was superior to both other temperature models (as well as north-side + area correction;  $\Delta AIC = 17.9$ ; Table 3). Among bootstrapped samples, 2,061 out of 10,000 model runs based on averaged phloem temperatures did better than the model using south-side temperatures with observed data, and only 206 of 10,000 north-side temperature models with area correction included did better (Table 3). These results suggest that when the von Foerster variant of the MPB

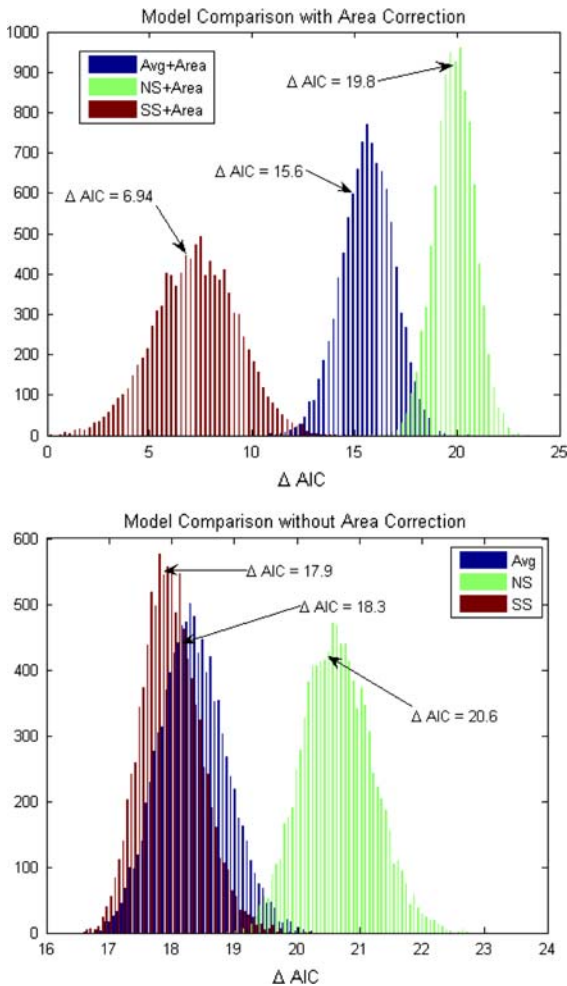


**Fig. 4** Comparison of changes in AIC among models using south-side (*SS*), north-side (*NS*) and averaged (*Avg*) phloem temperatures. Lower values of  $\Delta AIC$  correspond to better fits. In the top figure appear Comparisons among models with a logistic area correction are shown in the *top figure*. Model comparisons among models with only temperature are in the *bottom figure*. Locations of the  $\Delta AIC$  values for best fit models to actual data are indicated by *arrows* in each figure. Among models with logistic area correction, the analysis indicates that when south-side phloem temperatures are used model fit is slightly better than averaged temperatures, and north-side phloem temperatures provide the worst fit

phenology model is used, south-side phloem temperatures provide the best description of population growth rates, absent consideration of previously infested area.

To use these models in other areas and directly estimate model robustness, paired observations of phloem temperatures and ADS survey data are needed.

However, few records of phloem temperature measurements in other areas exist. Due to their relatively thin bark, north-side lodgepole pine phloem temperatures generally track hourly ambient air temperatures, with a slight thermal buffering effect for extreme lows (which are not developmentally significant). Therefore, in the absence of hourly south-side temperatures, which provided the best fit to observed data, hourly ambient air temperature would also provide a reasonable index of population success and outbreak potential (i.e.,  $r_n$ , net population growth rate).

In many cases, hourly ambient temperatures are also not available, although daily maximum and minimum ambient temperatures are. To test the performance of each model using daily maximum and minimum data, temperature inputs were created using ambient extrema connected with sine waves (placing minima at 6AM and maxima at 6PM). Predictions using the different models and the sinusoidal ambient temperatures were compared with both observations and model predictions using phloem temperatures for which each model was parameterized (Fig. 5). Models using south-side parameters outperformed the other four models. Averaged and north-side parameters provided increasingly poor performance in terms of percent variability explained ( $R^2$ ), with or without area correction (Fig. 5). Models using north-side or averaged temperature parameters and sinusoidal ambient temperatures over-predicted most annual growth rates, and predicted little of the annual variability. Ambient temperatures used in conjunction with south side-parameterized models performed somewhat better, describing slightly more than 50% of observed variability (Fig. 5).

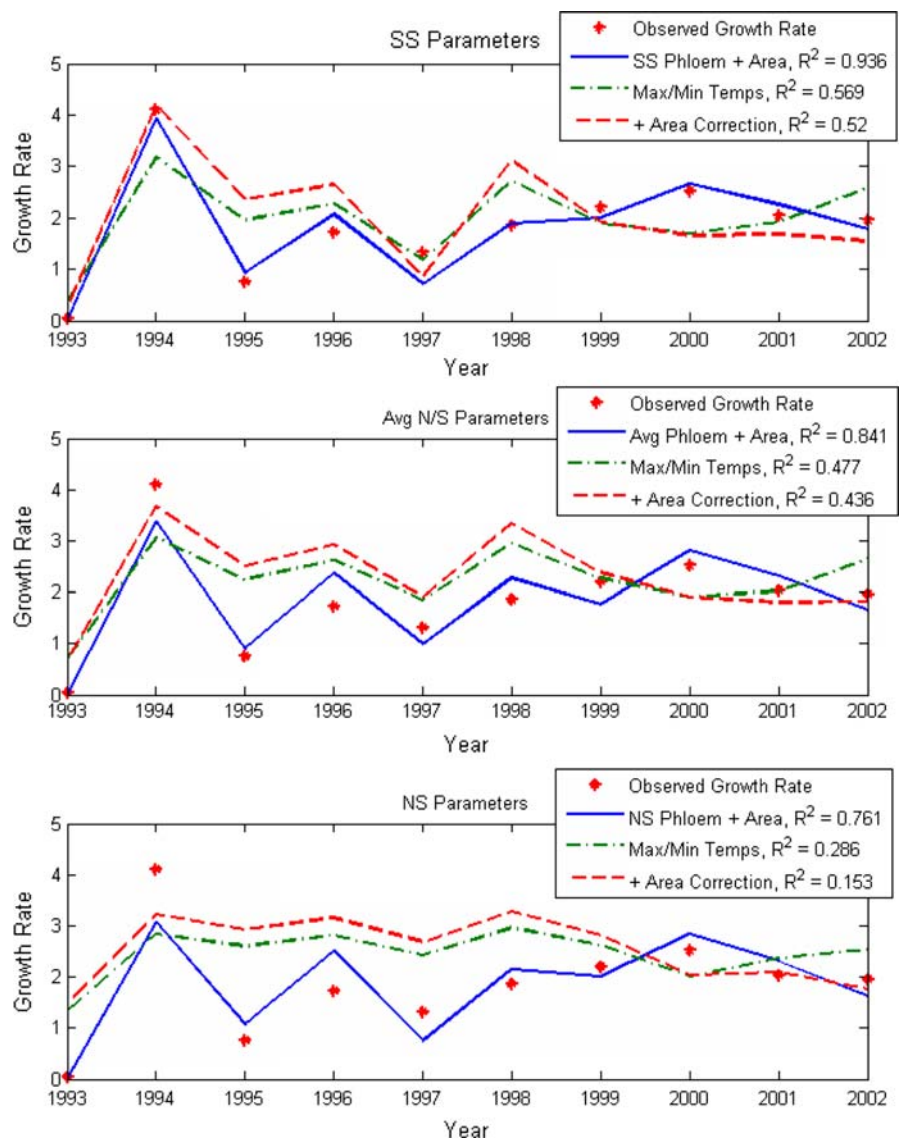
An alternative approach is linear interpolation connecting ambient extremes located at 6AM (minima) and 6PM (maxima), creating a saw-toothed temperature series. Comparison with observed values and optimal predictions for the models parameterized with various phloem temperatures appear in Fig. 6. Performance of all models is improved when compared with the sinusoidal temperature series, although models performed poorly when north-side and ambient temperatures were used. Similar to when sinusoidal temperatures were used, all models over-predicted growth rates when using saw-toothed temperatures. However, again, the model parameterized with south-side temperatures more convincingly reproduced fluctuations, capturing slightly more than two thirds

**Table 3** Comparison of models using change in AIC

Model	SS + area	Avg + area	NS + area	SS	Avg	NS
$\Delta$ AIC	6.94	15.6	19.8	17.9	18.3	20.6
$P$ [better than SS + area]	.45	0	0	0	0	0
$P$ [better than SS]	1.0	.96	.021	.46	.21	0

Each column corresponds to a phloem temperature (SS=south side, Avg=average, NS=north side) model; the first three columns are models with logistic area correction, the last three columns without. In the top row is the difference in AIC (from the minimum among all bootstrap samples) of the model fit to observed data. Shown in the second row are the number of samples of that model type which were better than the overall best model, SS + area. The zeros indicate that probability of outperforming the SS + area model is smaller than  $10^{-4}$  among bootstrapped alternatives. In the third row are fractions of runs (out of  $10^4$ ) performing better than a pure south side phloem temperature; e.g., the probability that an averaged temperature model would be better than the fitted south side model is smaller than 0.21

**Fig. 5** Predictions for MPB population growth rates in the SNRA study area using ambient daily maximum and minimum temperatures, connected with a sinusoidal curve. Predictions use parameters estimated using south-side (SS), averaged (Avg), and north-side (NS) phloem temperatures. Shown are predictions without correcting for area previously infested (*dash-dot line*), predictions using a logistic area correction for previously infested areas (*dashed line*), observed growth rates (\*), and model predictions based on observed phloem temperatures (*solid line*)



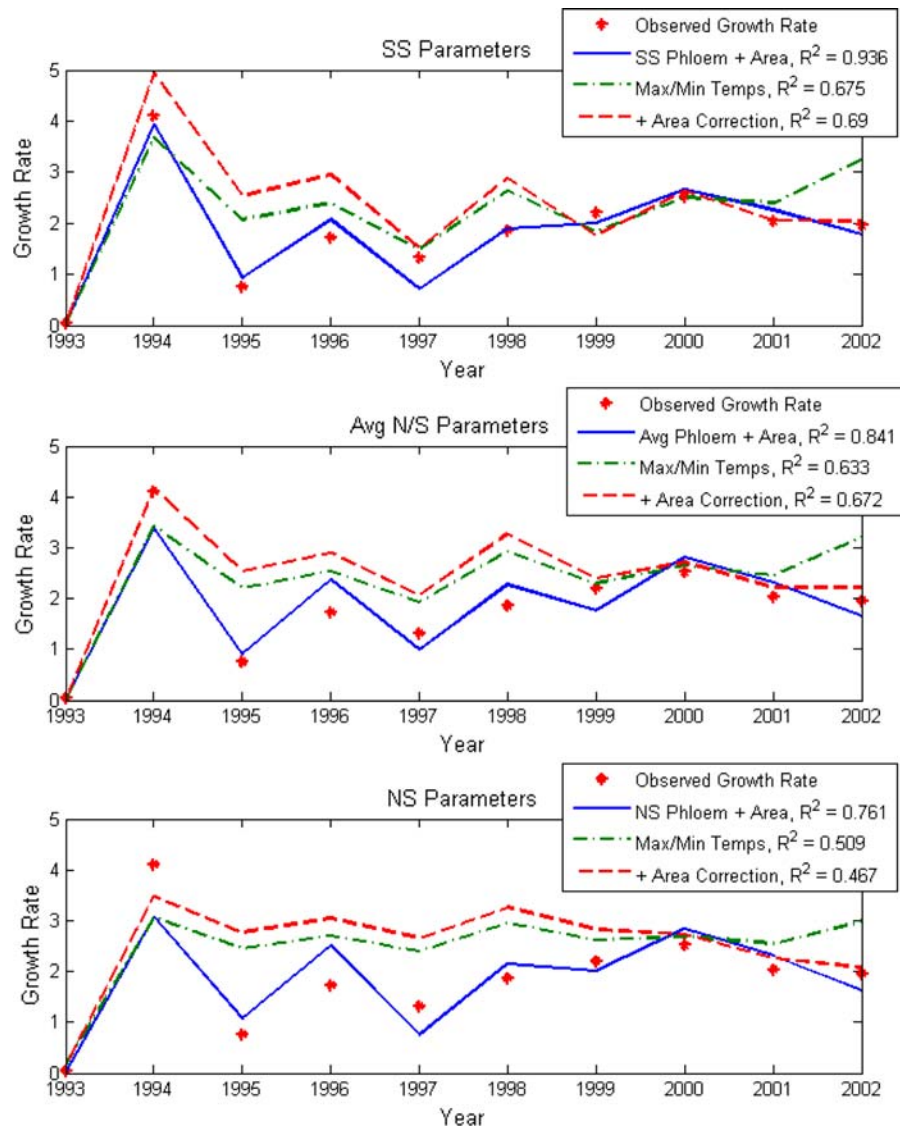


**Fig. 6** Predictions for MPB population growth rates in the SNRA study area using ambient daily maximum and minimum temperatures, connected linearly. Predictions used parameters estimated from south-side (SS), averaged (Avg), and north-side (NS) phloem temperatures. Shown are predictions without

correcting for area previously infested (*dash-dot line*), predictions using a logistic area correction for previously infested areas (*dashed line*), observed growth rates (\*), and model predictions based on observed phloem temperatures (*solid line*)

of the variability. Predictions using north-side models resulted in unrealistically large growth rates.

Overall, these results suggest that when the von Foerster variant of the MPB phenology is used, parameters estimated using south-side phloem temperatures and an area correction factor provide the best prediction of MPB population growth through time using either hourly phloem temperature or daily maximum and minimum ambient temperature.

## Discussion

The correspondence between models and observed MPB population growth rates in the SNRA study area were good, particularly for models including a correction for area previously infested by MPB. While the correlation coefficients suggest a degree of separation among the models depending on the temperature used, accounting for 60–90% of variability, when hourly

temperatures are used all of the models capture the basic fluctuations of population growth rates through the transition from pre-outbreak (before 1996) to outbreak (1996 and after). The models with area correction convincingly capture the decrease in growth rates as the outbreak transitioned into a host-limited post-outbreak phase. This suggests that the dynamical system

$$H_n = \alpha H_{n-1} E_n \cdot \exp\left(-\beta \sum_j^{n-1} H_j\right),$$

with parameters influenced by yearly temperature and phenology (through adjustments to the number of beetles rising above attack threshold on a typical tree,  $E_n$ ), is a good, simple description of infestation dynamics for MPB from the incipient to outbreak phase.

Differences among model parameters suggest that north-side temperatures (or ambient temperatures), when used with the von Foerster variant of the MPB phenology model, may not adequately describe the influence of phenology on outbreak dynamics. Our independent observations of attack density on trees in the SNRA provide estimates ranging from 150 to 200 attacking females per square meter, which would suggest 1,000 to 1,350 attacking females per tree (Powell and Bentz, unpublished data). These compare favorably only to parameters estimated using south-side temperature models, with or without area correction. All estimates for attacking MPB per tree produced using north-side temperatures are unrealistically high, between four and six thousand. Similarly, in the field we observed emergence of 1,200–1,500 MPB per square meter (Powell and Bentz, unpublished data), corresponding to 10,000 total emerging MPB as predicted by models using south-side temperatures. Model estimates when north-side temperatures were used were on the order of 25,000 emerging beetles, much higher than observed numbers.

To predict population growth in areas where hourly phloem temperatures are not available, hourly or daily maximum and minimum ambient temperatures may be used with reduced accuracy. Ambient temperatures predicted using a linear interpolation of daily maximum and minimum values in conjunction with south side-parameters provided the best fit to observed data.

## Conclusion

In this paper we have made a direct connection between highly variable temperature data, phenology expressed as adult emergence distributions based on the von Foerster variant of the MPB model, and growth rates of MPB populations at the landscape scale. Phenology affects the number of beetles which are ‘effective’ (that is, rising above a threshold required to successfully overwhelm new trees) by altering the degree of synchrony in emergence distributions. More tightly timed distributions result in more beetles over the critical threshold as compared with more dispersed distributions. Good predictions of variable growth rates through time are possible using hourly phloem temperatures from the south-side of host trees. A less precise reconstruction of growth rates can be generated using ambient hourly temperatures. Finally, ambient extrema, connected using sine-wave curves, does a good job of predicting population response using the parameters estimated with south-side phloem temperatures. The thermal models exhibit substantial improvement when an area correction term is included to adjust for previously infested area. This term decrements population growth rates by the growing improbability of finding a host which has not been previously attacked. Incorporating physiological responses to temperature into population dynamics models, as described here, offers the potential to greatly improve existing methods of risk prediction for MPB (Shore and Safranyik 1992; Bentz et al. 1993), and can be used to focus management and conservation activities.

**Acknowledgments** The authors wish to thank Nicholas Friedenbergh and two anonymous reviewers who gave helpful comments on an earlier version of the manuscript, as well as participants at the 2005 Snowbird Workshop, Bark Beetle Outbreaks in Western North America: Causes and Consequences, sponsored by the USDA Forest Service, Rapid Science Assessment Team, whose comments and thoughts helped formulate early stages of the modeling. Leslie Brown provided GIS support, which was very much appreciated.

## References

- Akaike H (1978) On the likelihood of a time series model. *Statistician* 27:217–235. doi:10.2307/2988185
- Alfaro R, Campbell R, Vera P, Hawkes B, Shore T (2004) Dendroecological reconstruction of mountain pine beetle outbreaks in the Chilcotin Plateau of British Columbia. In

- Shore TL, Brooks JE, Stone JE (eds) Mountain pine beetle symposium: challenges and solutions, Natural Resources Canada, Information Report BC-X-399, pp 245–256
- Amman GD, Cole WE (1983) Mountain pine beetle dynamics in lodgepole pine forests Part II: population dynamics. USDA For. Serv. Gen. Tech. Rpt. INT-145
- Anderson DR, Burnham KP, Thompson WL (2000) Null hypothesis testing: problems, prevalence and an alternative. *J Wildl Manag* 64:912–923. doi:[10.2307/3803199](https://doi.org/10.2307/3803199)
- Aukema BH, Carroll AL, Zhu J, Raffa KF, Sickely TA, Taylor SW (2006) Landscape level analysis of mountain pine beetle in British Columbia, Canada: spatiotemporal development and spatial synchrony within the present outbreak. *Ecogeography* 29:427–441. doi:[10.1111/j.2006.0906-7590.04445.x](https://doi.org/10.1111/j.2006.0906-7590.04445.x)
- Aukema BH, Carroll AL, Zheng Y, Zhu J, Raffa KF, Moore RD, Stahl K, Taylor SW (2008) Movement of outbreak populations of mountain pine beetle: influences of spatiotemporal patterns and climate. *Ecogeography* 31:348–358. doi:[10.1111/j.0906-7590.2007.05453.x](https://doi.org/10.1111/j.0906-7590.2007.05453.x)
- Bentz BJ (2006) Mountain pine beetle population sampling: inferences from Lindgren pheromone traps and tree emergence cages. *Can J For Res* 36(2):351–360. doi:[10.1139/x05-241](https://doi.org/10.1139/x05-241)
- Bentz BJ, Mullins DE (1999) Ecology of mountain pine beetle (Coleoptera: Scolytidae) cold hardening in the Intermountain west. *Environ Entomol* 28(4):577–587
- Bentz BJ, Logan JA, Amman GD (1991) Temperature dependent development of the mountain pine beetle (Coleoptera: Scolytidae), and simulation of its phenology. *Can Entomol* 123:1083–1094
- Bentz BJ, Amman GD, Logan JA (1993) A critical assessment of risk classification systems for the mountain pine beetle. *For Ecol Manag* 61:349–366. doi:[10.1016/0378-1127\(93\)90211-5](https://doi.org/10.1016/0378-1127(93)90211-5)
- Berryman AA, Stenseth NC, Wollkind DJ (1984) Metastability of forest ecosystems infested by bark beetles. *Res Popul Ecol (Kyoto)* 26(1):13–29. doi:[10.1007/BF02515505](https://doi.org/10.1007/BF02515505)
- Berryman AA, Raffa KF, Millstein JA, Stenseth NC (1989) Interaction dynamics of bark beetle aggregation and conifer defense rates. *Oikos* 56:256–263. doi:[10.2307/3565345](https://doi.org/10.2307/3565345)
- Borden JH (1974) Aggregation pheromones in the Scolytidae. In: Birch MC (ed) Pheromones. North-Holland Publishing Co., Amsterdam, pp 135–160
- Brody AK (1997) Effects of pollinators, herbivores, and seed predators on flowering phenology. *Ecology* 78:1624–1631
- Burnham KP, Anderson DR (2002) Model selection and multi-model inference: a practical information-theoretic approach, 2nd edn. Springer, New York 488 pp
- Calabrese JM, Fagan WF (2004) Lost in time, lonely and single: reproductive asynchrony and the Allee effect. *Am Nat* 164:25–37. doi:[10.1086/421443](https://doi.org/10.1086/421443)
- Carroll A, Taylor S, Regniere J, Safranyik L (2004) Effects of climate change on range expansion by the mountain pine beetle in British Columbia. In TL Shore, JE Brooks, JE Stone (eds) Mountain Pine Beetle Symposium: Challenges and Solutions, Natural Resources Canada, Information Report BC-X-399, pp. 223–232
- Crookston NL, Stark RW, Adams DL (1977) Outbreaks of mountain pine beetle in northwestern lodgepole pine forests—1945 to 1975. Forest, Wildlife and Range Experiment Station Bulletin No. 22. University of Idaho, Moscow, 7 pp
- Danks HV (1987) Insect dormancy: an ecological perspective. Monograph Series No. 1. Biological Survey of Canada (Terrestrial Arthropods), Ottawa
- Friedenberg NA, Powell JA, Ayres MP (2007) Synchrony's double edge: transient dynamics and the Allee effect in stage structured populations. *Ecol Lett* 10:564–573. doi:[10.1111/j.1461-0248.2007.01048.x](https://doi.org/10.1111/j.1461-0248.2007.01048.x)
- Gilbert E, Powell JA, Logan JA, Bentz BJ (2004) Comparison of three models predicting developmental milestones given environmental and individual variation. *Bull Math Biol* 66:1821–1850. doi:[10.1016/j.bulm.2004.04.003](https://doi.org/10.1016/j.bulm.2004.04.003)
- Heavilin J, Powell J (2008) A novel method of fitting spatio-temporal models to data, with applications to dynamics of mountain pine beetles. *Nat Resour Model* 21:489–524
- Hicke JA, Logan JA, Powell J, Ojima DS (2006) Changing temperatures influence suitability for modeled mountain pine beetle outbreaks in the western United States. *J Geophys Res* 11:GO2019. doi:[10.1029/2005JG000101](https://doi.org/10.1029/2005JG000101)
- Hunter AF, Elkinton JS (2000) Effects of synchrony with host plant on populations of a spring-feeding lepidopteran. *Ecology* 81:1248–1261
- IPCC (2007) Climate change 2007: the scientific basis. Contribution of working group I to the fourth assessment report of the Intergovernmental Panel on Climate Change. Cambridge University Press, Cambridge
- Lieutier F (2002) Mechanisms of resistance in conifers and bark beetle attack strategies. In: Wagner MR, Clancy KM, Lieutier F (eds) Mechanisms and deployment of resistance in trees to insects. Kluwer Academic Publishers, Boston, pp 31–78
- Logan JA, Bentz BJ (1999) Model analysis of mountain pine beetle (Coleoptera: Scolytidae) seasonality. *Environ Entomol* 28(6):924–934
- Logan JA, Powell JA (2001) Ghost forests, global warming, and the mountain pine beetle (Coleoptera: Scolytidae). *Am Entomol* 47(3):160–173
- Logan JA, White P, Bentz BJ, Powell JA (1998) Model analysis of spatial patterns in mountain pine beetle outbreaks. *Theor Popul Biol* 53:235–255. doi:[10.1006/tpbi.1997.1350](https://doi.org/10.1006/tpbi.1997.1350)
- Logan JA, Regniere J, Powell JA (2003) Assessing the impact of global warming on forest pest dynamics. *Front Ecol Environ* 1(3):130–137
- Logan JD, Wolesensky W, Joern A (2006) Temperature-dependent phenology and predation in arthropod systems. *Ecol Model* 196:471–482. doi:[10.1016/j.ecolmodel.2006.02.034](https://doi.org/10.1016/j.ecolmodel.2006.02.034)
- McGregor MD (1978) Status of mountain pine beetle Glacier National Park and Glacier View Ranger District, Flathead National Forest, MT, 1977. Forest insect and disease management report No. 78-6, Missoula
- Nelson WA, Lewis MA (2008) Connecting host physiology to host resistance in the conifer-bark beetle system. *Theor Ecol* 1:163–177
- Perkins DL, Swetnam TW (1996) A dendroecological assessment of whitebark pine in the Sawtooth-Salmon River region, Idaho. *Can J For Res* 26:2123–2133. doi:[10.1139/x26-241](https://doi.org/10.1139/x26-241)

- Post E, Levin SA, Iwasa Y, Stenseth NC (2001) Reproductive asynchrony increases with environmental disturbance. *Evol Int J Org Evol* 55:830–834. doi:[10.1554/0014-3820\(2001\)055\[0830:RAIWED\]2.0.CO;2](https://doi.org/10.1554/0014-3820(2001)055[0830:RAIWED]2.0.CO;2)
- Powell JA, Logan JA (2005) Insect seasonality—circle map analysis of temperature-driven life cycles. *Theor Popul Biol* 67:161–179. doi:[10.1016/j.tpb.2004.10.001](https://doi.org/10.1016/j.tpb.2004.10.001)
- Powell JA, Logan JA, Bentz BJ (1996) Local projections for a global model of mountain pine beetle attacks. *J Theor Biol* 179:243–260. doi:[10.1006/jtbi.1996.0064](https://doi.org/10.1006/jtbi.1996.0064)
- Powell J, Jenkins J, Logan J, Bentz BJ (2000) Seasonal temperature alone can synchronize life cycles. *Bull Math Biol* 62:977–998. doi:[10.1006/bulm.2000.0192](https://doi.org/10.1006/bulm.2000.0192)
- Raffa KF, Berryman AA (1983) The role of host plant resistance in the colonization behavior and ecology of bark beetles (Coleoptera: Scolytidae). *Ecol Monogr* 53:27–49. doi:[10.2307/1942586](https://doi.org/10.2307/1942586)
- Raffa KF, Phillips TW, Salom SM (1993) Strategies and mechanisms of host colonization by bark beetles. In: Schowalter TD, Filip GM (eds) *Beetle–pathogen interactions in conifer forests*. Academic Press, NY, pp 103–120
- Raffa KF, Aukema BH, Bentz BJ, Carroll AL, Hicke JA, Turner MG, Romme WH (2008) Cross-scale drivers of natural disturbances prone to anthropogenic amplification: dynamics of biome-wide bark beetle eruptions. *Bioscience* 58(6):501–518. doi:[10.1641/B580607](https://doi.org/10.1641/B580607)
- Rasmussen LA (1974) Flight and attack behavior of mountain pine beetles in lodgepole pine of northern Utah and southern Idaho. USDA For. Serv. Res. Note INT-180
- Régnière J, Bentz B (2007) Modeling cold tolerance in the mountain pine beetle, *Dendroctonus ponderosae*. *J Insect Physiol* 53:559–572. doi:[10.1016/j.jinsphys.2007.02.007](https://doi.org/10.1016/j.jinsphys.2007.02.007)
- Reid RW (1962a) Biology of the mountain pine beetle, *Dendroctonus monticolae* Hopkins, in the east Kootenay region of British Columbia: I. Life cycle, brood development, and flight periods. *Can Entomol* 94:531–538
- Reid RW (1962b) Biology of the mountain pine beetle, *Dendroctonus monticolae* Hopkins, in the east Kootenay region of British Columbia: II. Behaviour in the host, fecundity, and internal changes in the female. *Can Entomol* 94:605–613
- Safranyik L, Silversides R, McMullen LH, Linton DA (1989) An empirical approach to modeling local dispersal of the mountain pine beetle (*Dendroctonus ponderosae*) in relation to sources of attraction, wind direction, and speed. *J Appl Entomol* 108:498–511
- Safrayik L, Srimpton DM, Whitney HS (1975) An interpretation of the interaction between lodgepole pine, the mountain pine beetle and its associated blue stain fungi in western Canada. In Baumgartner DM (ed) *Management of Lodgepole pine ecosystems Symp. Proc.*, Washington State Univ. Cooperative Extension Service, pp. 406–428
- Shore TL, Safranyik L (1992) Susceptibility and risk rating systems for the mountain pine beetle in lodgepole pine stands. Inft. Rep. BC-X336, Pacific and Yukon Region. Forestry Canada, Pacific Forestry Centre, Victoria, 12 pp
- Tauber MJ, Tauber CA, Masaki S (1986) *Seasonal adaptations of insects*. Oxford University Press, New York
- Taylor F (1981) Ecology and evolution of physiological time in insects. *Am Nat* 117:1–23. doi:[10.1086/283683](https://doi.org/10.1086/283683)
- Xia JY, Rabbinge R, van der Werf W (2003) Multi stage functional responses in a Ladybeetle-Aphid system; scaling up from the laboratory to the field. *Environ Entomol* 32(1):151–162
- Zaslavski VA (1988) *Insect development: photoperiodic and temperature control*. Springer, Berlin